

Title: Constraining the Physics of Inflation

Date: Mar 06, 2012 02:30 PM

URL: <http://pirsa.org/12030106>

Abstract:

Observational constraints on the physics of inflation

Kendrick Smith (Princeton)
Perimeter Institute, March 2012

Outline

Inflation overview

Non-Gaussian models

CMB phenomenology and statistics

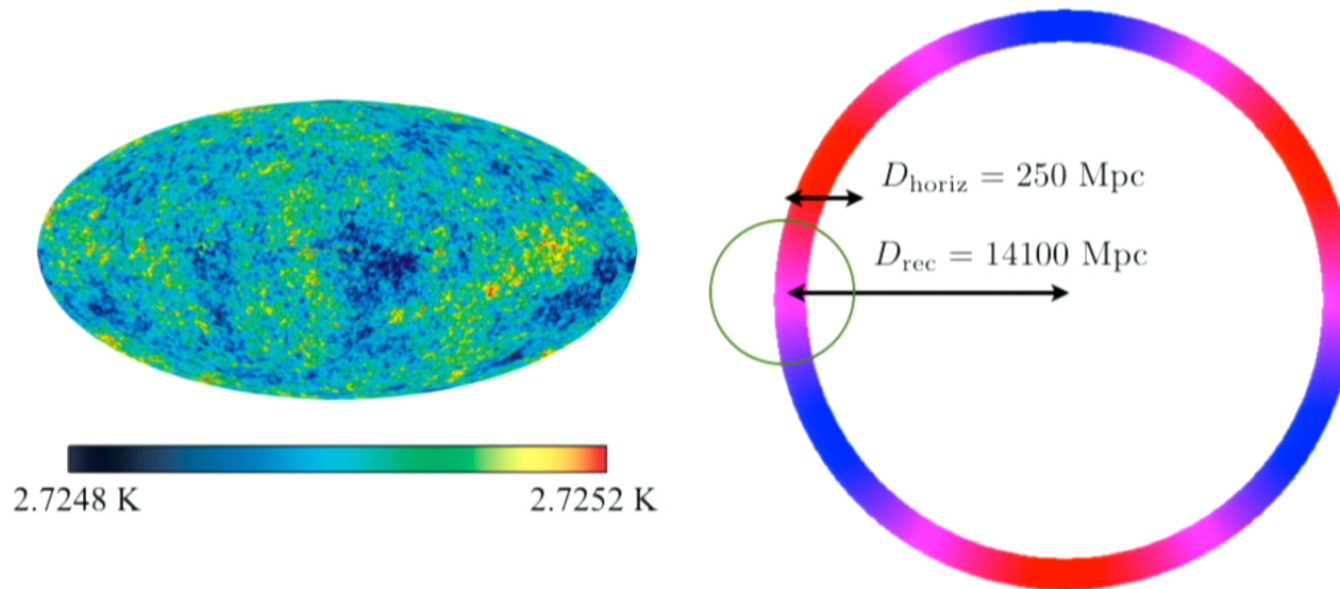
WMAP results

Large-scale structure

Horizon problem

Surface of last scattering is nearly **isothermal**, suggesting that all parts of the last scattering surface were once in causal contact

However, the causal horizon at last scattering is much smaller: points separated by $> 1^\circ$ have **never been in causal contact**



Horizon problem

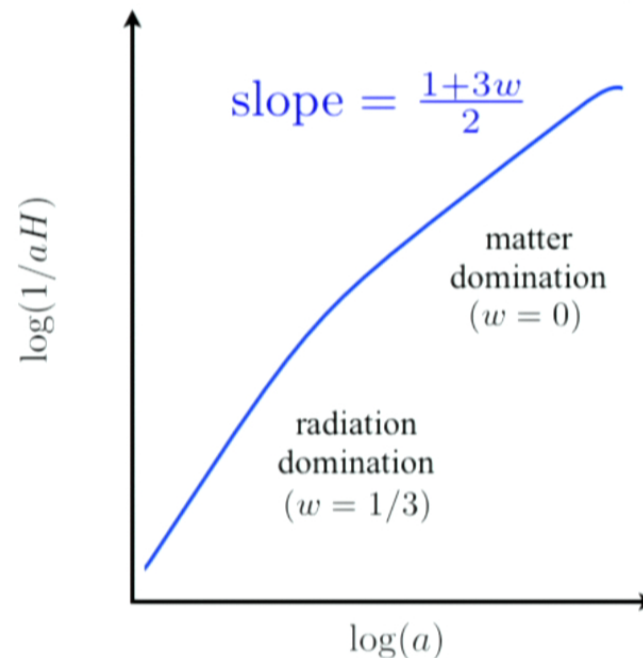
$(aH)^{-1}$ = comoving distance light travels in an e-folding

Evolution with scale factor a :

$$\frac{d \log(aH)^{-1}}{d \log a} = \frac{1 + 3w}{2}$$

$$(w = \frac{\text{pressure}}{\text{energy density}})$$

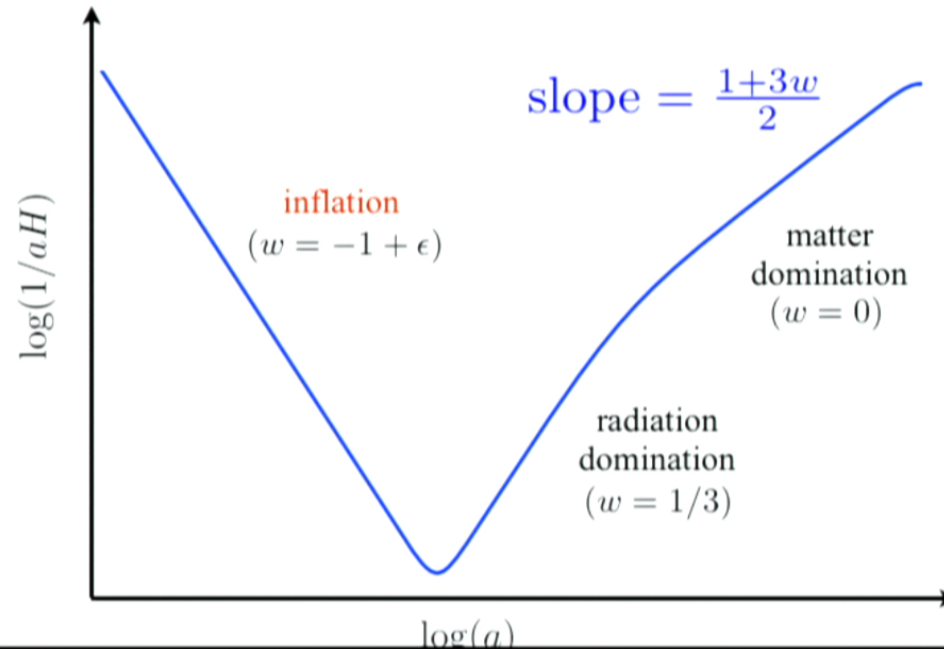
In a universe filled with
nonrelativistic ($w = 0$)
or relativistic ($w = 1/3$)
matter, the horizon is
small at early times



Inflation

To get a large horizon at early times, Λ CDM expansion history must be preceded by an “inflationary” epoch with $w < -\frac{1}{3}$, i.e. negative pressure

$$(w = \frac{\text{pressure}}{\text{energy density}})$$




Generation of perturbations

Amazing fact: inflation naturally generates perturbations

In an expanding background, microscopic degrees of freedom are quantum mechanically excited


Toy example: massless test scalar field ($-\infty < \tau < 0$)

$$S = \frac{1}{2} \int d\tau d^3x a(\tau)^2 \left[\left(\frac{d\sigma}{d\tau} \right)^2 - (\partial_i \sigma)^2 \right]$$


time dependence

Each Fourier mode $\sigma_{\mathbf{k}}$ behaves as a 1D harmonic oscillator with **time dependent Hamiltonian**

$$\hat{H} = \frac{1}{2} \left[\frac{k^2}{(H\tau)^2} \hat{x}^2 + (H\tau)^2 \hat{p}^2 \right]$$


 σ_k conjugate momentum

Generation of perturbations

Consider time-dependent Hamiltonian $\hat{H} = \frac{1}{2} \left(\frac{k^2}{(H\tau)^2} \hat{x}^2 + (H\tau)^2 \hat{p}^2 \right)$

Schrodinger equation $i \frac{\partial \psi}{\partial \tau} = \hat{H} \psi$ is **exactly solvable**:

$$\psi(x, \tau) \propto \frac{1}{(1 - ik\tau)^{1/2}} \underbrace{e^{-i \frac{k\tau}{2} - i \frac{k^2 x^2}{2H^2 \tau (1 + k^2 \tau^2)}}}_{\text{phase}} \underbrace{\exp \left(- \frac{k^3 x^2}{2H^2 (1 + k^2 \tau^2)} \right)}_{\text{Gaussian}}$$

Early-time limit ($\tau \ll -1/k$): system stays in ground state (adiabatic)

$$\psi(x, \tau) \rightarrow \psi_{\text{ground}}(x, \tau) \propto \exp \left(- \frac{kx^2}{2H^2 \tau^2} \right)$$

Late-time limit ($\tau \gg -1/k$): wavefunction “frozen” to constant value

$$\psi(x, \tau) \rightarrow \exp \left(- \frac{k^3 x^2}{2H^2} \right)$$

At the end of inflation, the scalar field $\sigma_{\mathbf{k}}$ is a **Gaussian field** with **scale-invariant power spectrum** $\langle \sigma_{\mathbf{k}} \sigma_{\mathbf{k}'}^* \rangle = \frac{H^2}{2k^3} (2\pi)^3 \delta^3(\mathbf{k} - \mathbf{k}')$

Generation of perturbations

Analogously to the test scalar, (almost) all fields are quantum mechanically excited (e.g. gravitational waves are generated)

One more ingredient: **reheating** (fluctuations in inflationary sector convert to fluctuations in Standard Model particles)

Simplest scenario: initial perturbation is “adiabatic”, generated entirely by inflation fluctuations

$$ds^2 = -dt^2 + a(t)^2 e^{2\zeta(x,t)} dx^2$$

“adiabatic curvature”

Non-Gaussianity is **unobservably small** (Maldacena 2002), given the following assumptions:

1. single-field (initial fluctuations come only from inflaton)
2. reheating is homogeneous
3. inflaton Lagrangian is $\frac{1}{2}(\partial\phi)^2 - V(\phi)$

Generation of perturbations

Analogously to the test scalar, (almost) all fields are quantum mechanically excited (e.g. gravitational waves are generated)

One more ingredient: **reheating** (fluctuations in inflationary sector convert to fluctuations in Standard Model particles)

Simplest scenario: initial perturbation is “adiabatic”, generated entirely by inflation fluctuations

$$ds^2 = -dt^2 + a(t)^2 e^{2\zeta(x,t)} dx^2$$

“adiabatic curvature”

Non-Gaussianity is **unobservably small** (Maldacena 2002), given the following assumptions:

1. single-field (initial fluctuations come only from inflaton)
2. reheating is homogeneous
3. inflaton Lagrangian is $\frac{1}{2}(\partial\phi)^2 - V(\phi)$

A non-Gaussian model: modulated reheating

Suppose that the decay rate Γ of the inflaton is **not constant**, but controlled by an auxiliary field σ :

$$\Gamma(\mathbf{x}) = \Gamma_0 + \Gamma_1 \sigma(\mathbf{x}) + \Gamma_2 \sigma(\mathbf{x})^2 + \dots$$

This generates a curvature fluctuation after the inflaton decays (regions which decay later undergo more expansion):

$$\zeta(\mathbf{x}) = A(\delta\sigma(\mathbf{x})) + B(\delta\sigma(\mathbf{x}))^2 + \dots$$

Suppose σ is a **Gaussian field** (via the standard quantum mechanical mechanism). After a trivial change of variables:

$$\zeta(\mathbf{x}) = \zeta_G(\mathbf{x}) + \frac{3}{5} f_{NL}^{\text{loc}} \zeta_G(\mathbf{x})^2 + \dots$$

where ζ_G is a Gaussian field and f_{NL}^{loc} is a free parameter.

A non-Gaussian model: modulated reheating

Suppose that the decay rate Γ of the inflaton is **not constant**, but controlled by an auxiliary field σ :

$$\Gamma(\mathbf{x}) = \Gamma_0 + \Gamma_1 \sigma(\mathbf{x}) + \Gamma_2 \sigma(\mathbf{x})^2 + \dots$$

This generates a curvature fluctuation after the inflaton decays (regions which decay later undergo more expansion):

$$\zeta(\mathbf{x}) = A(\delta\sigma(\mathbf{x})) + B(\delta\sigma(\mathbf{x}))^2 + \dots$$

Suppose σ is a **Gaussian field** (via the standard quantum mechanical mechanism). After a trivial change of variables:

$$\zeta(\mathbf{x}) = \zeta_G(\mathbf{x}) + \frac{3}{5} f_{NL}^{\text{loc}} \zeta_G(\mathbf{x})^2 + \dots$$

where ζ_G is a Gaussian field and f_{NL}^{loc} is a free parameter.

Non-Gaussianity: “local model”

$$\zeta(\mathbf{x}) = \zeta_G(\mathbf{x}) + \frac{3}{5} f_{NL}^{\text{loc}} \zeta_G(\mathbf{x})^2 \quad \leftarrow \text{non-Gaussian}$$

Arises if non-G is generated by **local physics after horizon crossing**

- modulated reheating (inflaton decay mediated by spectator field)
- curvaton model (spectator field with non-flat potential generates ζ)
- “New” Ekpyrosis (two-field model; second field generates ζ)

Natural values in these models: $f_{NL}^{\text{loc}} = 1\text{--}100$

$$\begin{aligned} \Delta f_{NL}^{\text{loc}} &= 21 \text{ (WMAP7)} \\ \text{Observational errors (1}\sigma\text{): } \Delta f_{NL}^{\text{loc}} &\approx 5 \text{ (Planck)} \\ \Delta f_{NL}^{\text{loc}} &\approx 1 \text{ (LSST)} \end{aligned}$$

Local non-Gaussianity requires multiple fields; observation of $f_{NL}^{\text{loc}} \neq 0$ would **rule out all single-field models**

Non-Gaussianity via cubic interactions

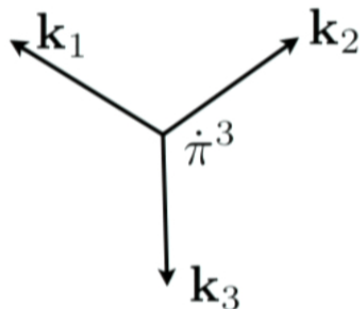
Add interaction terms to the Lagrangian

Toy example: massless test scalar with $\dot{\sigma}^3$ interaction

$$S = \frac{1}{2} \int d\tau d^3x a(\tau)^2 \left[\left(\frac{\partial \sigma}{\partial \tau} \right)^2 - (\partial_i \sigma)^2 \right] + f a(\tau) \left(\frac{\partial \sigma}{\partial \tau} \right)^3$$

small coupling constant

To first order in f , non-Gaussianity shows up in the **3-point function**



$$\begin{aligned} \langle \sigma_{\mathbf{k}_1} \sigma_{\mathbf{k}_2} \sigma_{\mathbf{k}_3} \rangle &\propto f \int_{-\infty}^0 d\tau \frac{\tau^2 e^{(k_1 + k_2 + k_3)\tau}}{k_1 k_2 k_3} \\ &= \frac{2f}{k_1 k_2 k_3 (k_1 + k_2 + k_3)^3} \end{aligned}$$

Non-Gaussianity via cubic interactions

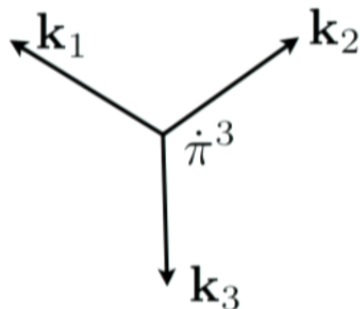
Add interaction terms to the Lagrangian

Toy example: massless test scalar with $\dot{\sigma}^3$ interaction

$$S = \frac{1}{2} \int d\tau d^3x a(\tau)^2 \left[\left(\frac{\partial \sigma}{\partial \tau} \right)^2 - (\partial_i \sigma)^2 \right] + f a(\tau) \left(\frac{\partial \sigma}{\partial \tau} \right)^3$$

small coupling constant

To first order in f , non-Gaussianity shows up in the **3-point function**



$$\begin{aligned} \langle \sigma_{\mathbf{k}_1} \sigma_{\mathbf{k}_2} \sigma_{\mathbf{k}_3} \rangle &\propto f \int_{-\infty}^0 d\tau \frac{\tau^2 e^{(k_1 + k_2 + k_3)\tau}}{k_1 k_2 k_3} \\ &= \frac{2f}{k_1 k_2 k_3 (k_1 + k_2 + k_3)^3} \end{aligned}$$

Non-Gaussianity in single-field inflation

Classification theorem: if

1. the inflaton is the source of the initial curvature perturbations
2. no rapid explicit time dependence (e.g. oscillatory potentials)
3. coefficients are “generic” (i.e. no special symmetries)

Then the most general curvature 3-point function is:

$$\langle \zeta_{\mathbf{k}_1} \zeta_{\mathbf{k}_2} \zeta_{\mathbf{k}_3} \rangle = f_{\dot{\sigma}^3} F_{\dot{\sigma}^3}(k_1, k_2, k_3) + f_{\dot{\sigma}(\partial\sigma)^2} F_{\dot{\sigma}(\partial\sigma)^2}(k_1, k_2, k_3)$$

where $F_{\dot{\sigma}^3} =$ 3-point function of test scalar with $\dot{\sigma}^3$ interaction

$$\propto \frac{1}{k_1 k_2 k_3 (k_1 + k_2 + k_3)^3}$$

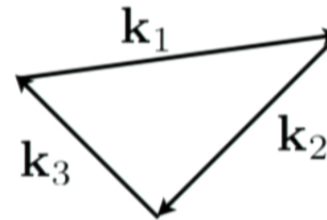
$F_{\dot{\sigma}(\partial\sigma)^2} =$ 3-point function of test scalar with $\dot{\sigma}(\partial_i\sigma)^2$ interaction

$$\propto \frac{(4k_1^2 + 6k_1 k_2 + 6k_1 k_3 + k_3^2)(k_1 \cdot k_2)}{k_1^3 k_2^3 k_3 (k_1 + k_2 + k_3)^3} + \text{perm.}$$

Senatore, Smith & Zaldarriaga 2009

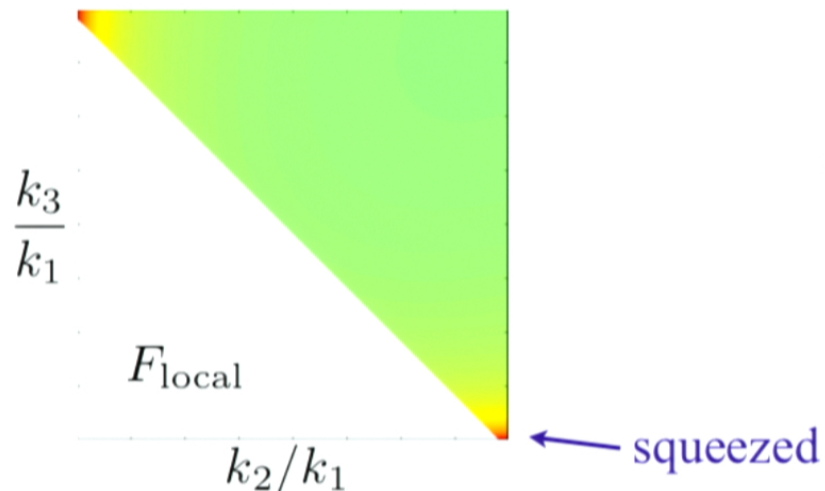
“Shapes” of non-Gaussianity

Curvature 3-point function $\langle \zeta_{\mathbf{k}_1} \zeta_{\mathbf{k}_2} \zeta_{\mathbf{k}_3} \rangle$
defined for **closed triangles**, depends
only on shape of triangle



To visualize, plot $k_2^2 k_3^2 \langle \zeta_{\mathbf{k}_1} \zeta_{\mathbf{k}_2} \zeta_{\mathbf{k}_3} \rangle$ vs side ratios (k_2/k_1) , (k_3/k_1)

Local shape $\langle \zeta_{\mathbf{k}_1} \zeta_{\mathbf{k}_2} \zeta_{\mathbf{k}_3} \rangle = \frac{6}{5} f_{NL}^{\text{loc}} P_\zeta(k_1) P_\zeta(k_2) + \text{cyc.}$



Signal-to-noise dominated
by **squeezed triangles**



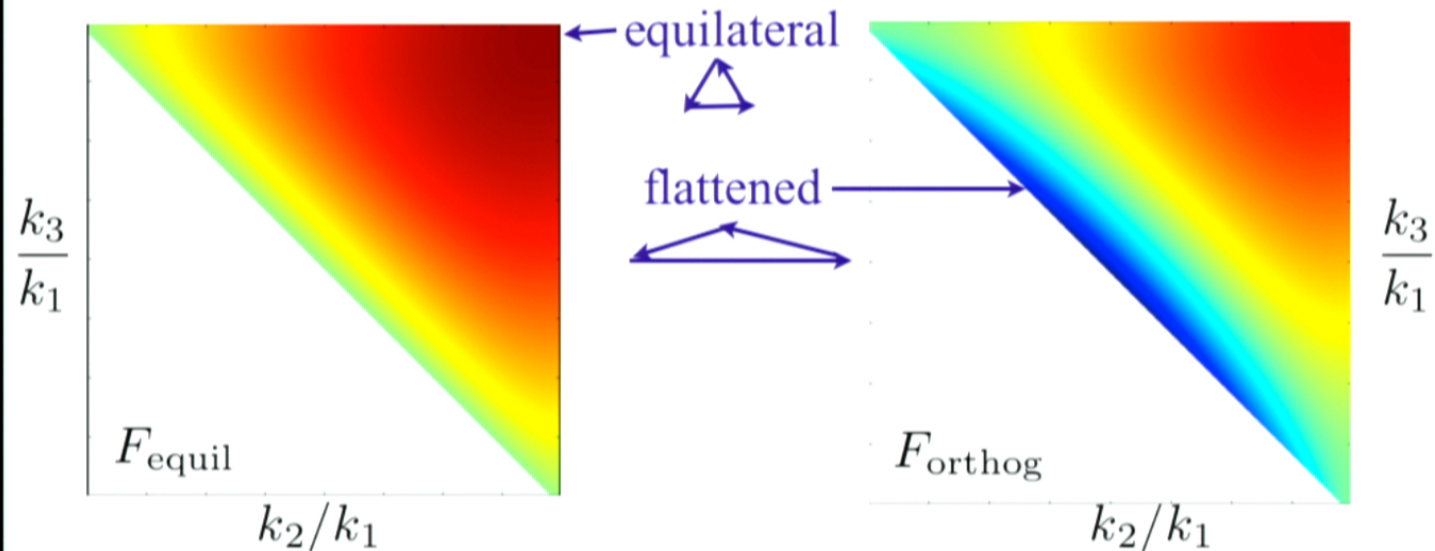
“Shapes” of non-Gaussianity

Single-field shapes $F_{\dot{\sigma}^3}(k_1, k_2, k_3)$, $F_{\dot{\sigma}(\partial\sigma)^2}(k_1, k_2, k_3)$
are very similar (highly correlated)

Orthogonalize: define new basis

$$F_{\text{equil}} = 1.21 F_{\dot{\sigma}^3} + 1.04 F_{\dot{\sigma}(\partial\sigma)^2}$$

$$F_{\text{orthog}} = 0.108 F_{\dot{\sigma}^3} - 0.068 F_{\dot{\sigma}(\partial\sigma)^2}$$



Senatore, Smith & Zaldarriaga 2009

Outline

Inflation overview

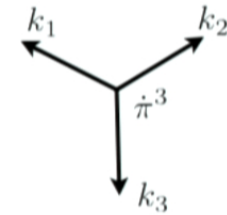
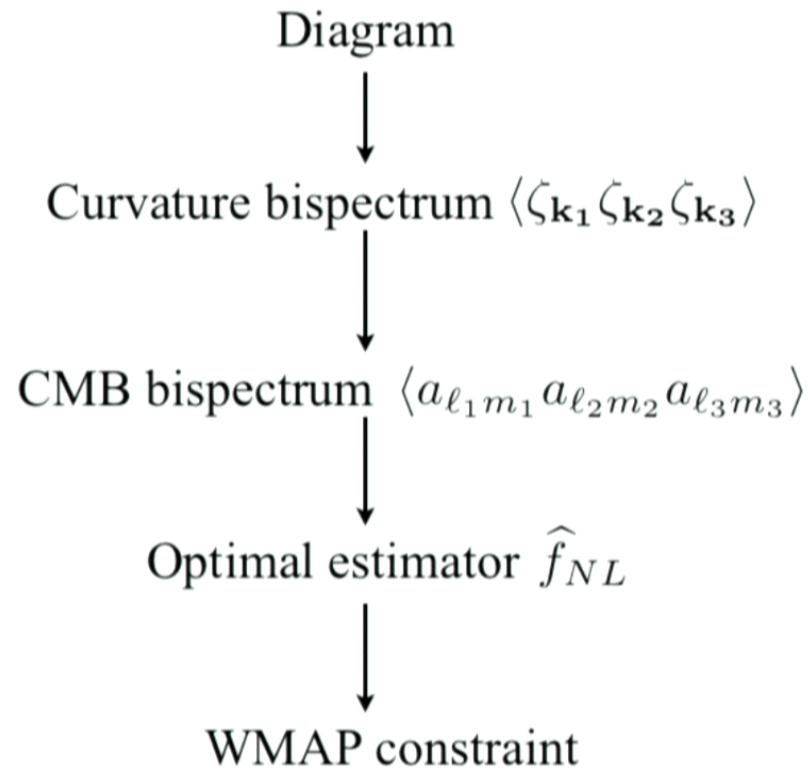
Non-Gaussian models

CMB phenomenology and statistics

WMAP results

Large-scale structure

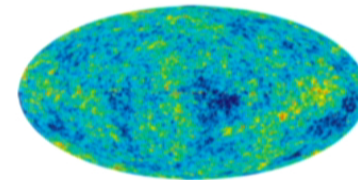
Data analysis



$$\int d\eta \frac{\eta^2 e^{-(k_1+k_2+k_3)\eta}}{k_1 k_2 k_3}$$

$$\sqrt{\frac{\prod (2\ell_i + 1)}{4\pi}} \int d\eta dr \eta^2 r^2 \prod \mu_{\ell_i}(\eta, r) \times \begin{pmatrix} \ell_1 & \ell_2 & \ell_3 \\ 0 & 0 & 0 \end{pmatrix} \begin{pmatrix} \ell_1 & \ell_2 & \ell_3 \\ m_1 & m_2 & m_3 \end{pmatrix}$$

$$\int \eta^2 d\eta \int r^2 dr \int \left(\sum_{\ell m} \mu_{\ell}(\eta, r) (C^{-1}a)_{\ell m} \right)^3$$



General case is computationally intractable

Calculating CMB bispectrum from curvature bispectrum:

$$\langle a_{\ell_1 m_1} a_{\ell_2 m_2} a_{\ell_3 m_3} \rangle = \sqrt{\frac{(2\ell_1 + 1)(2\ell_2 + 1)(2\ell_3 + 1)}{4\pi}} \begin{pmatrix} \ell_1 & \ell_2 & \ell_3 \\ 0 & 0 & 0 \end{pmatrix} \begin{pmatrix} \ell_1 & \ell_2 & \ell_3 \\ m_1 & m_2 & m_3 \end{pmatrix} \\ \times \int dr dk_1 dk_2 dk_3 \left(\prod_{i=1}^3 \frac{2k_i^2}{\pi} j_{\ell_i}(k_i r) \Delta_{\ell_i}(k_i) \right) \langle \zeta_{\mathbf{k}_1} \zeta_{\mathbf{k}_2} \zeta_{\mathbf{k}_3} \rangle$$

CMB transfer function (computed numerically)

4D oscillatory integral for each (ℓ_1, ℓ_2, ℓ_3) : too slow

Computing optimal estimator from data $(a_{\ell m})$:

$$\hat{f}_{NL} = \sum_{\ell_i m_i} \langle a_{\ell_1 m_1} a_{\ell_2 m_2} a_{\ell_3 m_3} \rangle (C^{-1}a)_{\ell_1 m_1} (C^{-1}a)_{\ell_2 m_2} (C^{-1}a)_{\ell_3 m_3}$$

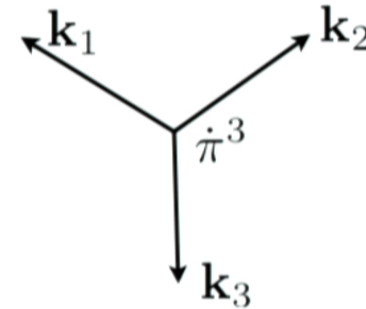
Number of terms in sum is $\approx \ell_{\max}^5$: too slow

Smith & Zaldarriaga (2007)

Physical shapes are tractable!

Example: $\dot{\pi}^3$ interaction

$$\langle \zeta_{\mathbf{k}_1} \zeta_{\mathbf{k}_2} \zeta_{\mathbf{k}_3} \rangle \propto \int_{-\infty}^0 d\tau \frac{\tau^2 e^{(k_1+k_2+k_3)\tau}}{k_1 k_2 k_3}$$

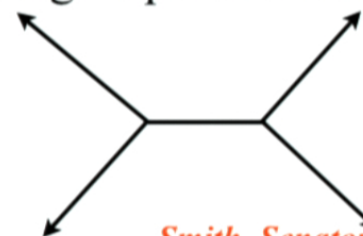
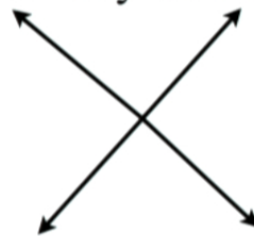


Specialized to this case, estimator can be written in tractable form:

$$\hat{f}_{NL} = \int \tau^2 d\tau \int r^2 dr \int d^2 \mathbf{n} \left(\sum_{\ell m} \mu_{\ell}(\tau, r) (C^{-1} a)_{\ell m} Y_{\ell m}(\mathbf{n}) \right)^3$$

$$\mu_{\ell}(\tau, r) = \int \frac{2k dk}{\pi} j_{\ell}(kr) e^{\tau k} \Delta_{\ell}(k)$$

Generalizes to any **tree diagram**, e.g. 4-point estimators:



Smith, Senatore & Zaldarriaga, to appear

Computational problem 1: large number of terms

$$\hat{f}_{NL} = \sum_i \tau_i^2(\Delta\tau) \sum_j r_j^2(\Delta r) \int d^2\mathbf{n} \left(\sum_{\ell m} \mu_{\ell}(\tau_i, r_j) (C^{-1}a)_{\ell m} Y_{\ell m}(\mathbf{n}) \right)^3$$

Sum of many terms, corresponding to points in (τ, r) plane

Proposed **optimization algorithm** to reduce computational cost

General form:

Given estimator $\hat{X} = \sum_{i=1}^N \hat{X}_i$ and covariance matrix $\text{Cov}(\hat{X}_i, \hat{X}_j)$

Find minimal (in sense defined by Cov) subset $\{\hat{X}_{i_1}, \hat{X}_{i_2}, \dots, \hat{X}_{i_M}\}$

Original \hat{X} can be written w/fewer terms: $w_1 \hat{X}_{i_1} + \dots + w_M \hat{X}_{i_M}$

Specialized to \hat{f}_{NL} : Start with many points in the (τ, r) plane

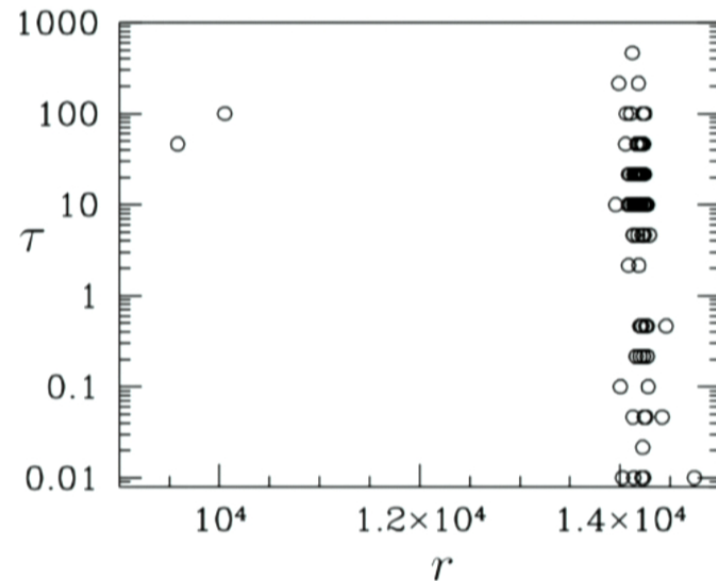
Optimization algorithm gives small number of points, weights

Optimization algorithm: example

$$\hat{f}_{NL} = \int \tau^2 d\tau \int r^2 dr \int d^2\mathbf{n} \left(\sum_{\ell m} \mu_{\ell}(\tau, r) (C^{-1}a)_{\ell m} Y_{\ell m}(\mathbf{n}) \right)^3$$

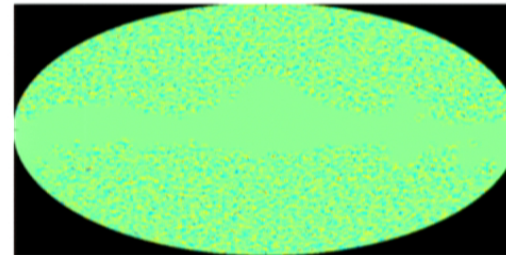
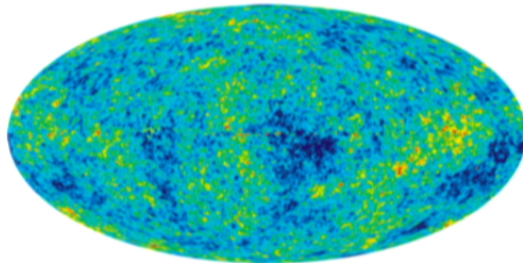
“Unoptimized” estimator: 80000 terms corresponding to dense sampling in the (τ, r) plane

Applying optimization algorithm reduces number of integration points (or terms in the estimator) to **86**



Smith & Zaldarriaga (2007)

Computational problem 2: C^{-1}



CMB map = vector a

$$C^{-1}a = (S + N)^{-1}a$$

N = Noise covariance matrix (diagonal in pixel space)

S = Signal covariance matrix (diagonal in harmonic space)

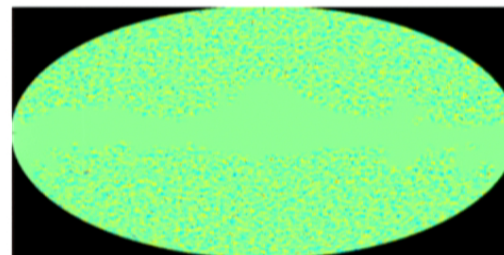
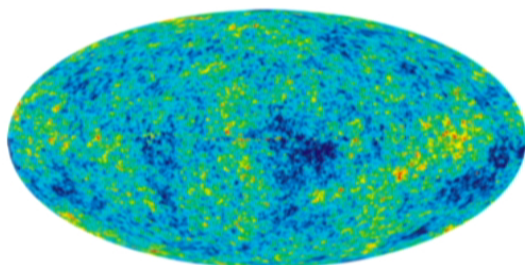
Appears to require inverting 10^6 -by- 10^6 matrix!

Proposed **fast multigrid algorithm** for solving $(S + N)x = a$
iteratively (similar to elliptic PDE such as $\nabla^2 x = a$)

Enables many types of optimal statistics (e.g. optimal C_ℓ)

Smith, Zahn, Doré & Nolte 2008

Computational problem 2: C^{-1}



CMB map = vector a

$$C^{-1}a = (S + N)^{-1}a$$

N = Noise covariance matrix (diagonal in pixel space)

S = Signal covariance matrix (diagonal in harmonic space)

Appears to require inverting 10^6 -by- 10^6 matrix!

Proposed **fast multigrid algorithm** for solving $(S + N)x = a$
iteratively (similar to elliptic PDE such as $\nabla^2 x = a$)

Enables many types of optimal statistics (e.g. optimal C_ℓ)

Smith, Zahn, Doré & Nolte 2008

Outline

Inflation overview

Non-Gaussian models

CMB phenomenology and statistics

WMAP results

Large-scale structure

WMAP results: local shape

First optimal analysis: $f_{NL}^{\text{loc}} = 38 \pm 21$ (1σ)

(Smith, Senatore & Zaldarriaga 2009)

At the time, results in the literature were difficult to interpret...

$$f_{NL}^{\text{loc}} = 32 \pm 34 \quad (\text{Creminelli et al})$$

$$f_{NL}^{\text{loc}} = 87 \pm 30 \quad (\text{Yadav \& Wandelt})$$

$$f_{NL}^{\text{loc}} = 55 \pm 30 \quad (\text{Komatsu et al})$$

Optimal estimator achieves smallest error bars and **ensures uniqueness of result** by removing “choices” in data analysis

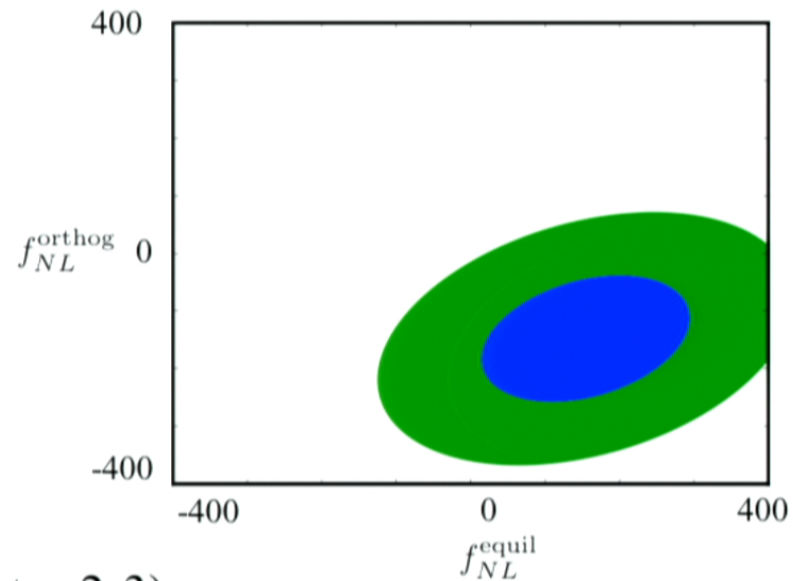
Current data is consistent with single-field inflation ($f_{NL}^{\text{loc}} = 0$);
Planck will reduce error bar by factor ~ 4

WMAP results: single-field shapes

First optimal constraints:

$$f_{NL}^{\text{equil}} = 155 \pm 140$$

$$f_{NL}^{\text{orthog}} = -149 \pm 110$$



(Planck: errors smaller by factor 2-3)

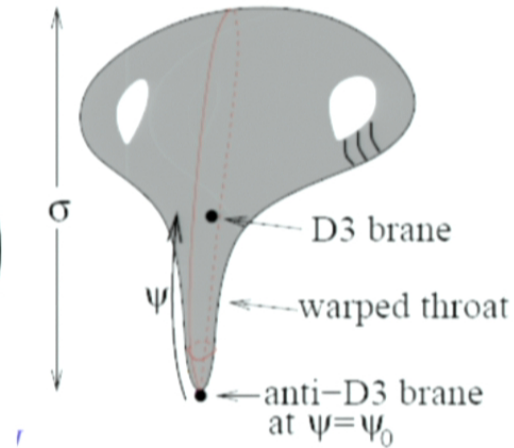
“Master result” which can be compared to all single-field models

Senatore, Smith & Zaldarriaga 2009

Case study: DBI inflation

String-motivated model of inflation
(Alishahiha, Silverstein & Tong)

$$\mathcal{L} = -\frac{1}{g_s} \left(\frac{\sqrt{1 + f(\phi)(\partial\phi)^2}}{f(\phi)} + V(\phi) \right)$$



Single field model, classification theorem applies....

$$f_{NL}^{\text{equil}} = -\frac{0.35}{c_s^2} \quad f_{NL}^{\text{orthog}} = -\frac{0.024}{c_s^2}$$

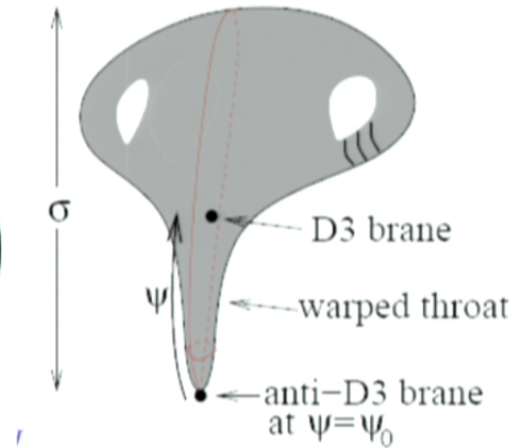
From WMAP results we get: $c_s \gtrsim 0.054$ (95% CL)

Senatore, Smith & Zaldarriaga 2009

Case study: DBI inflation

String-motivated model of inflation
(Alishahiha, Silverstein & Tong)

$$\mathcal{L} = -\frac{1}{g_s} \left(\frac{\sqrt{1 + f(\phi)(\partial\phi)^2}}{f(\phi)} + V(\phi) \right)$$



Single field model, classification theorem applies....

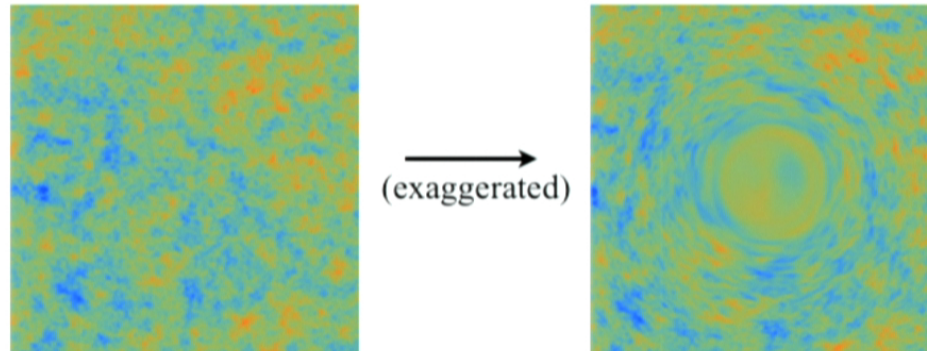
$$f_{NL}^{\text{equil}} = -\frac{0.35}{c_s^2} \quad f_{NL}^{\text{orthog}} = -\frac{0.024}{c_s^2}$$

From WMAP results we get: $c_s \gtrsim 0.054$ (95% CL)

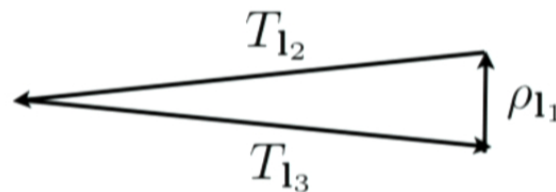
Senatore, Smith & Zaldarriaga 2009

WMAP results: gravitational lensing

Apparent locations of CMB hot and cold spots are deflected by intervening large scale structure



Generates squeezed 3-point function $\langle \rho_{1_1} T_{1_2} T_{1_3} \rangle$
where ρ = projected matter density

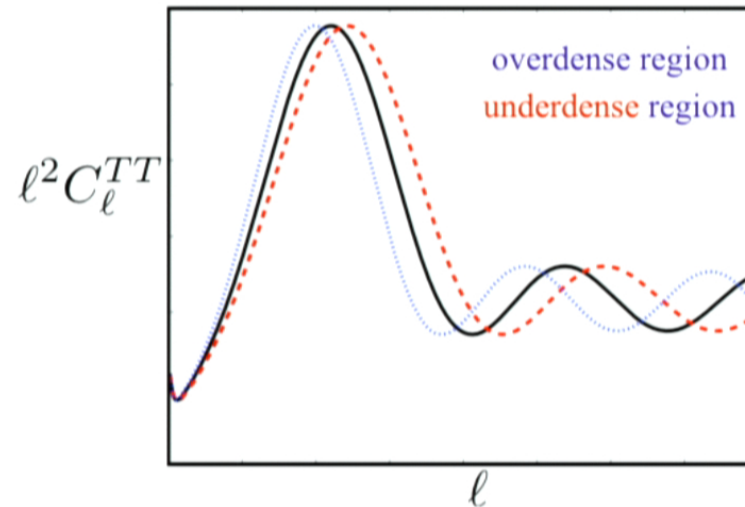
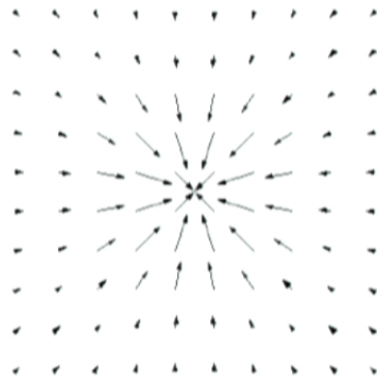


Smith, Zahn, Doré & Nolte 2008

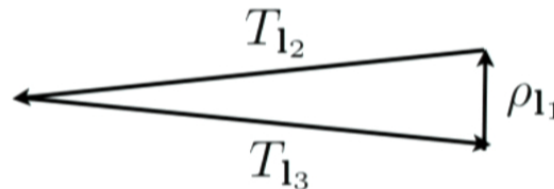
WMAP results: gravitational lensing

Consider a large (~ 10 deg) overdense region

CMB appears slightly magnified; acoustic peaks move to lower l



Correlation between long-wavelength density ρ and small-scale CMB power spectrum C_ℓ^{TT} is equivalent to a three-point correlation



WMAP results: gravitational lensing

NVSS: 1.4 GHz all-sky radio survey

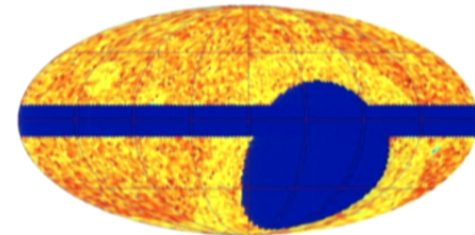
Use galaxy counts as tracer for
projected matter density



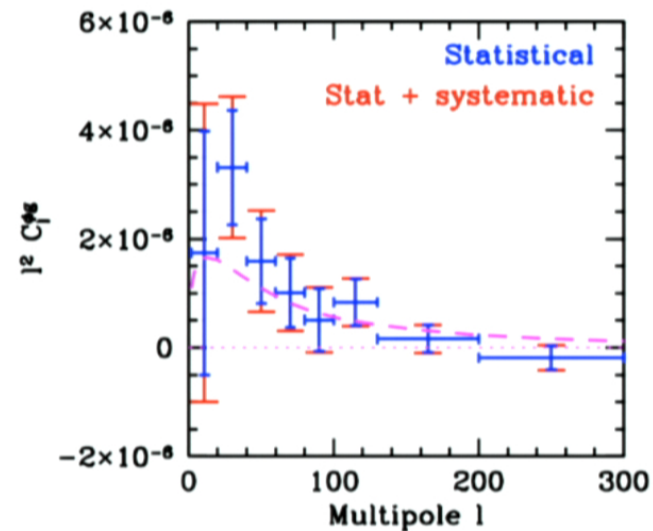
Three-point signal detected at 3.4σ
First detection of CMB lensing!

Will soon enter realm of precision
cosmology, e.g. 30σ in Planck

Smith, Zahn, Doré & Nolte 2008



galaxy counts (Galactic coordinates)



Outline

Inflation overview

Non-Gaussian models

CMB phenomenology and statistics

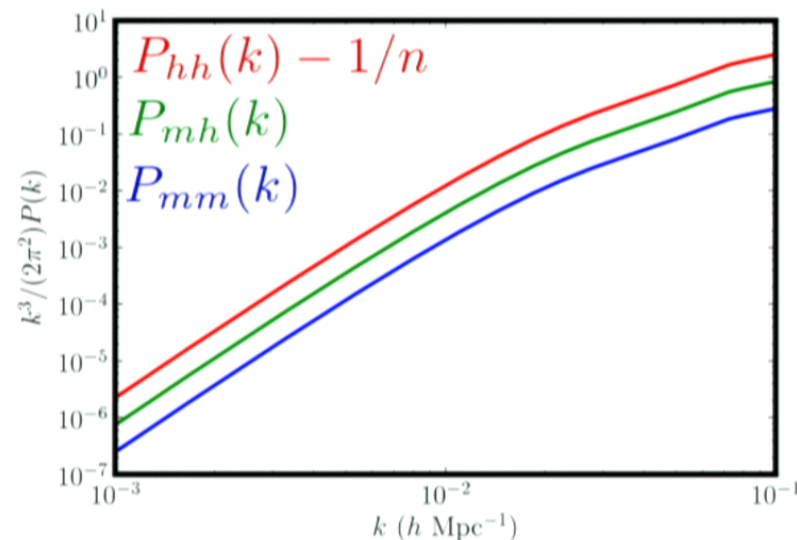
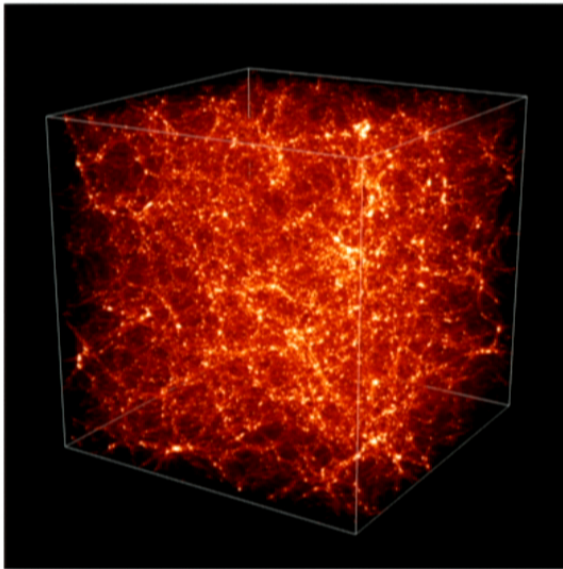
WMAP results

Large-scale structure

Large-scale structure: halo bias

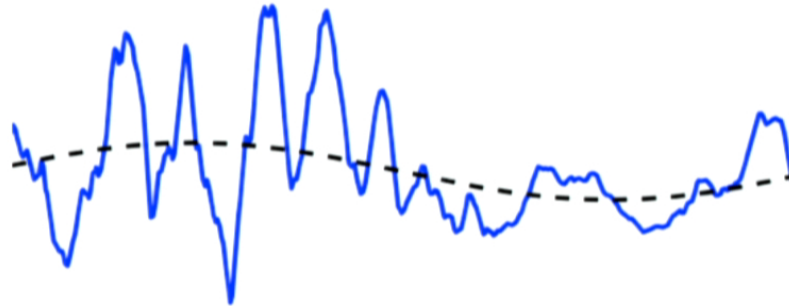
In a **Gaussian cosmology**, halo number density is proportional to the dark matter density on large scales: $\frac{\delta\rho_h}{\bar{\rho}_h} \approx b \frac{\delta\rho_m}{\bar{\rho}_m}$ **b = “halo bias”**

Matter-halo power spectrum P_{mh} and halo-halo power spectrum P_{hh} are proportional to matter power spectrum $P_{mm}(k)$



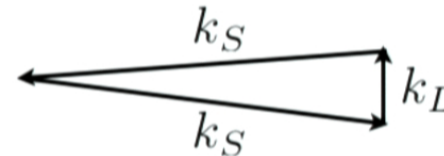
Interpretation

Correlation between long-wavelength mode and small-scale power



Three-point function is large in **squeezed triangles**

$$\langle \zeta_{\mathbf{k}_L} \zeta_{\mathbf{k}_S} \zeta_{\mathbf{k}_S} \rangle \propto f_{NL} \frac{1}{k_L^3 k_S^3}$$

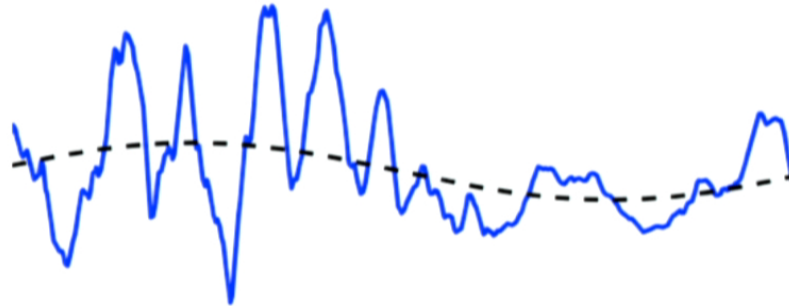


Locally measured fluctuation amplitude σ_8^{loc} near a point \mathbf{x} depends on value of Newtonian potential $\Phi(\mathbf{x})$

$$\sigma_8^{\text{loc}} = \bar{\sigma}_8 (1 + 2f_{NL}\Phi)$$

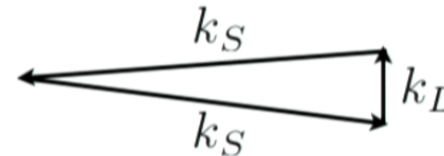
Interpretation

Correlation between long-wavelength mode and small-scale power



Three-point function is large in **squeezed triangles**

$$\langle \zeta_{\mathbf{k}_L} \zeta_{\mathbf{k}_S} \zeta_{\mathbf{k}_S} \rangle \propto f_{NL} \frac{1}{k_L^3 k_S^3}$$

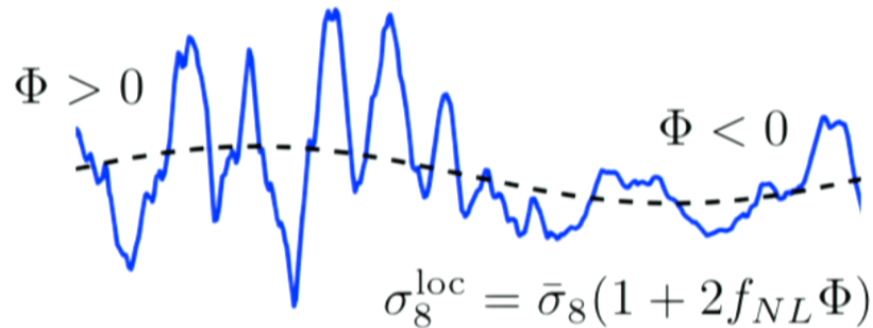


Locally measured fluctuation amplitude σ_8^{loc} near a point \mathbf{x} depends on value of Newtonian potential $\Phi(\mathbf{x})$

$$\sigma_8^{\text{loc}} = \bar{\sigma}_8 (1 + 2f_{NL}\Phi)$$

Interpretation

This picture naturally leads to **enhanced large-scale clustering**

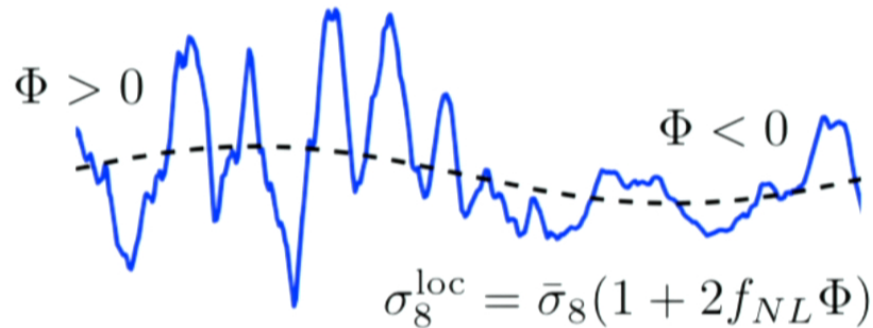


$$\rho_h = \bar{\rho}_h \left(1 + \underbrace{\frac{\partial \log \rho_h}{\partial \log \rho_m}}_{b_0} \frac{\delta \rho_m}{\bar{\rho}_m} + \underbrace{\frac{\partial \log \rho_h}{\partial \log \sigma_8}}_{b_1/2} \frac{\delta \sigma_8}{\bar{\sigma}_8} \right)$$

$$\begin{aligned} \frac{\delta \rho_h}{\bar{\rho}_h} &= b_0 \frac{\delta \rho_m}{\bar{\rho}_m} + b_1 f_{NL} \Phi \\ &= \left(b_0 + b_1 \frac{f_{NL}}{(k/aH)^2} \right) \frac{\delta \rho_m}{\bar{\rho}_m} \end{aligned}$$

Interpretation

This picture naturally leads to **enhanced large-scale clustering**



$$\rho_h = \bar{\rho}_h \left(1 + \underbrace{\frac{\partial \log \rho_h}{\partial \log \rho_m}}_{b_0} \frac{\delta \rho_m}{\bar{\rho}_m} + \underbrace{\frac{\partial \log \rho_h}{\partial \log \sigma_8}}_{b_1/2} \frac{\delta \sigma_8}{\bar{\sigma}_8} \right)$$

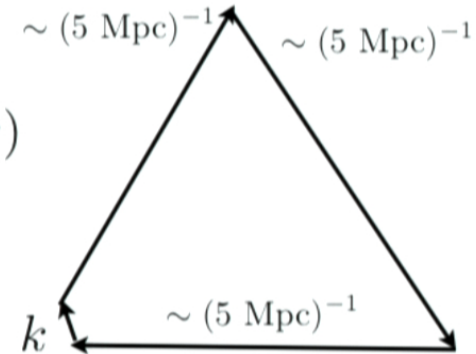
$$\begin{aligned} \frac{\delta \rho_h}{\bar{\rho}_h} &= b_0 \frac{\delta \rho_m}{\bar{\rho}_m} + b_1 f_{NL} \Phi \\ &= \left(b_0 + b_1 \frac{f_{NL}}{(k/aH)^2} \right) \frac{\delta \rho_m}{\bar{\rho}_m} \end{aligned}$$

General expression for non-Gaussian clustering

Schematic form:

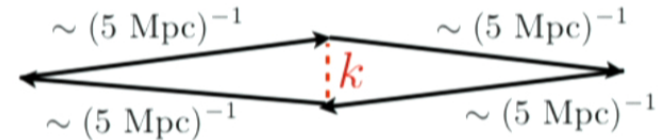
$$P_{mh}(k) = \left(b_0 + \sum_{N=1}^{\infty} b_N f_{N+2}(k) \right) P_{mm}(k)$$

$$f_N(k) = \int_{\mathbf{k}_i} \langle \zeta_{\mathbf{k}} \zeta_{\mathbf{k}_1} \cdots \zeta_{\mathbf{k}_{N-1}} \rangle$$



$$P_{hh}(k) = \left(b_0^2 + 2 \sum_{N=1}^{\infty} b_0 b_N f_{N+2}(k) + \sum_{MN} b_M b_N g_{M+1,N+1}(k) \right) P_{mm}(k)$$

$$g_{MN}(k) = \int_{\substack{\sum \mathbf{k}_i = \mathbf{k} \\ \sum \mathbf{k}'_j = -\mathbf{k}}} \langle \zeta_{\mathbf{k}_1} \cdots \zeta_{\mathbf{k}_M} \zeta_{\mathbf{k}'_1} \cdots \zeta_{\mathbf{k}'_N} \rangle$$

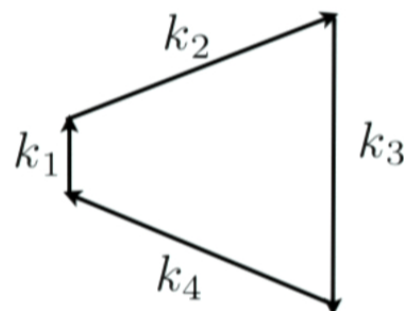


in prep. with Baumann, Green and Ferraro

Example 1: bias from 4-point function

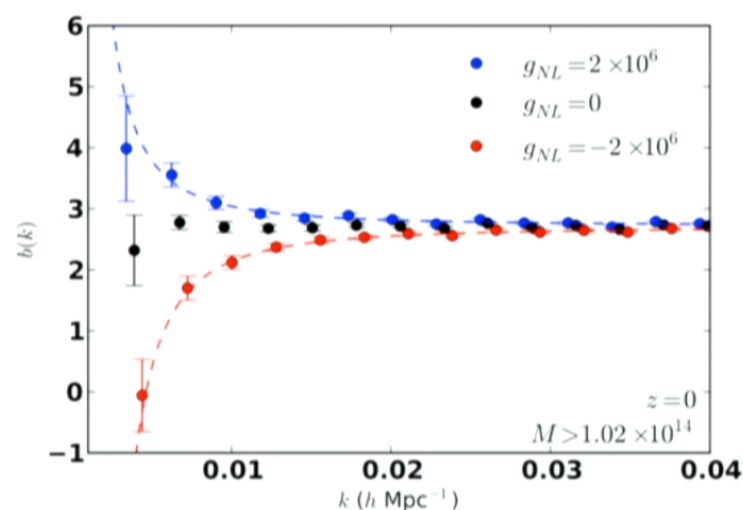
Simple example of non-Gaussian model
whose 4-point function $\langle \zeta_{\mathbf{k}_1} \zeta_{\mathbf{k}_2} \zeta_{\mathbf{k}_3} \zeta_{\mathbf{k}_4} \rangle$
is large in the limit $k_1 \rightarrow 0$:

$$\zeta = \zeta_G + g_{NL} \zeta_G^3$$



Large-scale clustering signatures
are qualitatively similar to f_{NL}^{loc}
model

Detailed **mass, redshift and scale
dependence** agree well with
general expression

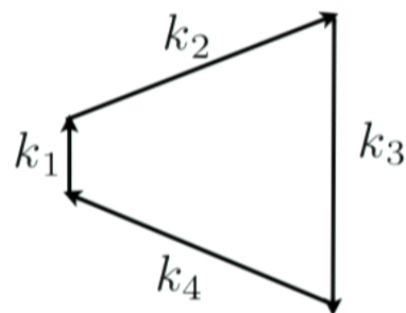


Smith, Ferraro & LoVerde 2011

Example 1: bias from 4-point function

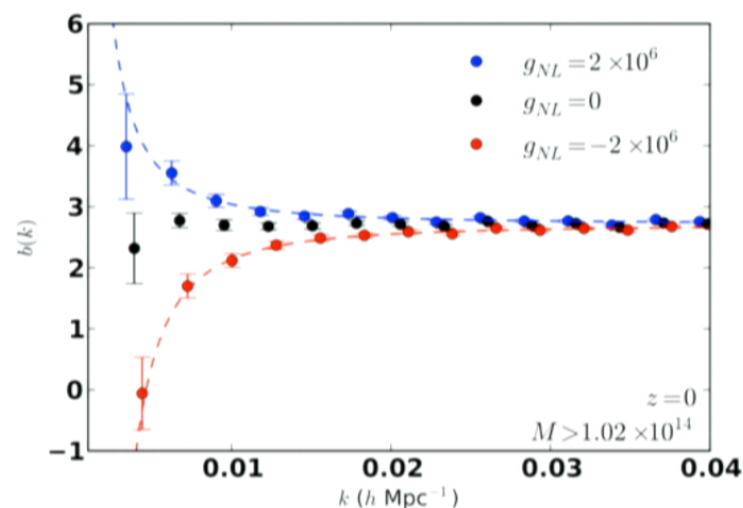
Simple example of non-Gaussian model
whose 4-point function $\langle \zeta_{\mathbf{k}_1} \zeta_{\mathbf{k}_2} \zeta_{\mathbf{k}_3} \zeta_{\mathbf{k}_4} \rangle$
is large in the limit $k_1 \rightarrow 0$:

$$\zeta = \zeta_G + g_{NL} \zeta_G^3$$



Large-scale clustering signatures
are qualitatively similar to f_{NL}^{loc}
model

Detailed **mass, redshift and scale
dependence** agree well with
general expression



Smith, Ferraro & LoVerde 2011

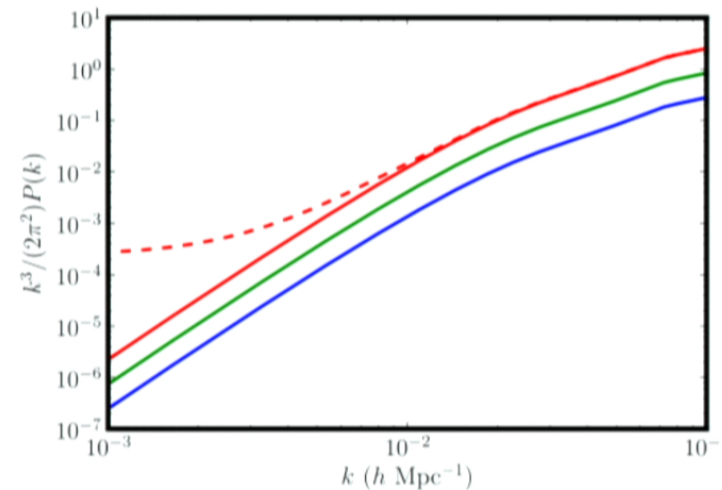
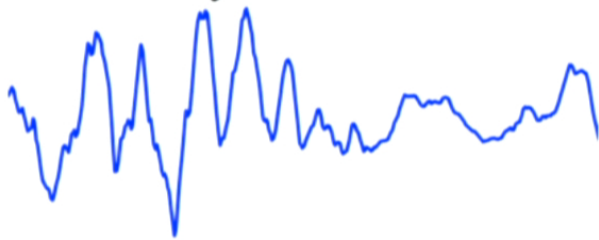
Example 2: “stochastic” halo bias

Simple example of model such that $\langle \zeta_{\mathbf{k}_1} \zeta_{\mathbf{k}_2} \zeta_{\mathbf{k}_3} \rangle = 0$, but $\langle \zeta_{\mathbf{k}_1} \zeta_{\mathbf{k}_2} \zeta_{\mathbf{k}_3} \zeta_{\mathbf{k}_4} \rangle$ is large in limit $|\mathbf{k}_1 + \mathbf{k}_2| \rightarrow 0$:

$$\zeta = \zeta_G + f \zeta_G \zeta'_G$$

Leads to “stochastic” clustering:
non-Gaussian excess in P_{hh}
but not P_{mh}

σ_8 has long-wavelength
fluctuations, but uncorrelated
with density

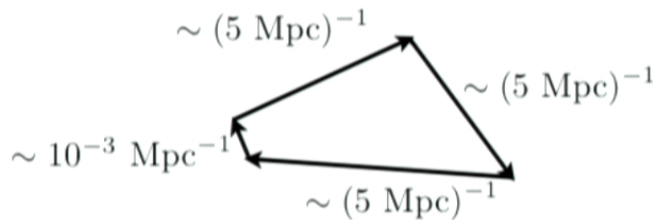


Smith & LoVerde 2010

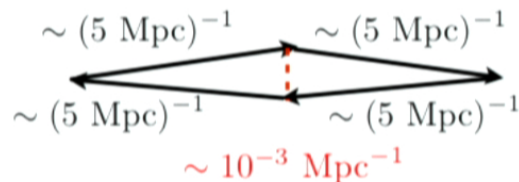
Large-scale structure: general picture

Large-scale structure constraints are best understood as precise tests of **statistical homogeneity of the universe on large scales**

Non-Gaussian models with large squeezed limits can be interpreted as **large-scale inhomogeneity in statistics of small-scale modes**, e.g:



large-scale correlation
between **density** and
small-scale skewness

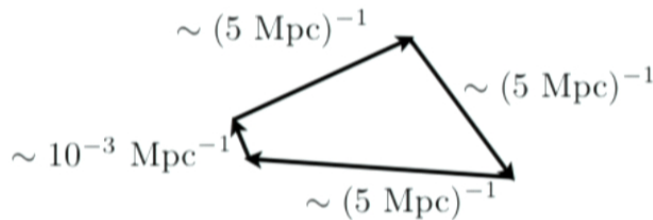


large-scale inhomogeneity
in **small-scale power**,
uncorrelated to density
("stochastic")

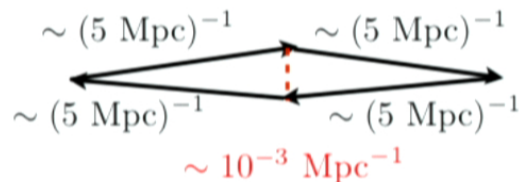
Large-scale structure: general picture

Large-scale structure constraints are best understood as precise tests of **statistical homogeneity of the universe on large scales**

Non-Gaussian models with large squeezed limits can be interpreted as **large-scale inhomogeneity in statistics of small-scale modes**, e.g:



large-scale correlation
between **density** and
small-scale skewness



large-scale inhomogeneity
in **small-scale power**,
uncorrelated to density
("stochastic")

Conclusions and future outlook

Theory:

Primordial non-Gaussianity is a powerful, multifaceted probe of early universe physics. Can map QFT interactions to observable signals

Do we have a complete set of signals to look for?
No; new examples are still emerging...

- single-field: higher derivative interactions

Behbahani, Mirbabayi, Senatore & Smith in prep.

- multi-field: “SUSY shapes”

Chen & Wang 0911.3380

Baumann & Green 1109.0292

Baumann, Green, Ferraro & Smith in prep.

Conclusions and future outlook

CMB phenomenology:

Can measure N-point correlation function $\langle T_{l_1} T_{l_2} \cdots T_{l_N} \rangle$ with full shape discrimination. “One estimator per diagram”

Optimal data analysis requires solving several algorithmic and computational problems; when dust settled, WMAP data is consistent with Gaussian statistics

Many shapes remain to be analyzed!

- higher derivative cubic interactions
- four-point statistics / quartic interactions
- “SUSY shapes”

Planck will dramatically improve existing constraints (Jan 2013!) but it will be **difficult to improve further using the CMB**

Conclusions and future outlook

Large-scale structure:

- Future constraints on many models (e.g. f_{NL}^{loc}) better than CMB

Caveat: difficult to separate different N-point shapes
(or separate different values of N)

Caveat: LSS is not sensitive to all parameters (e.g. f_{NL}^{equil})

- Subject still in its infancy; many basic problems unsolved
How can we simulate random initial conditions (e.g. for an N-body simulation) from an arbitrary interacting QFT?

Smith & Brown in prep.

Is the large-scale galaxy power spectrum the best observable?

LoVerde & Smith in prep.

- We are still quite far from the ultimate limits on our ability to constrain inflation; the near future will bring many new theoretical and observational results!